

Phosphors for X-ray detectors in computed tomography

W. Rosner and B.C. Grabmaier

Research and Corporate Research and Development, Applied Materials Research, Otto-Neta-Ring 6, 8080 München EA, Germany

One of the most attractive applications of phosphors is their use as X-ray conversion detectors in X-ray computed tomography (CT), the dominating method of medical radiology. The principle of CT is described and the resulting requirements for general phosphors are derived. The properties of submicrocrystalline phosphors are reviewed. Finally, the recent developments of a new class of phosphors based on ceramic of rare earth compounds are discussed.

1. Introduction

One of the most attractive applications of phosphors is their use as X-ray conversion detectors for diagnostic systems in medical radiology. In addition, nuclear medical imaging systems such as gamma-camera, positron emitting tomography and single photon emission tomography utilize phosphors for scintillation counting detectors.

In medical radiology imaging systems, classic intensifying-screens and aspirable tubes, as well as recently developed image phosphors for digitized

radiography are widely used to visualize X-ray transmission generated structures of the human body. However, within the last two decades a completely new diagnostic method has been established in this field, it is known as X-ray computed tomography (CT). Now, CT holds an eminent position due to the possibility of generating cross-sectional images of the interior of the human body with extraordinary quality. For example, the high quality image CT in Fig. 1 shows cross-sectional scans of the abdomen (fig. 1(a)) and the head (base of the skull, fig. 1(b)). Without entering into the

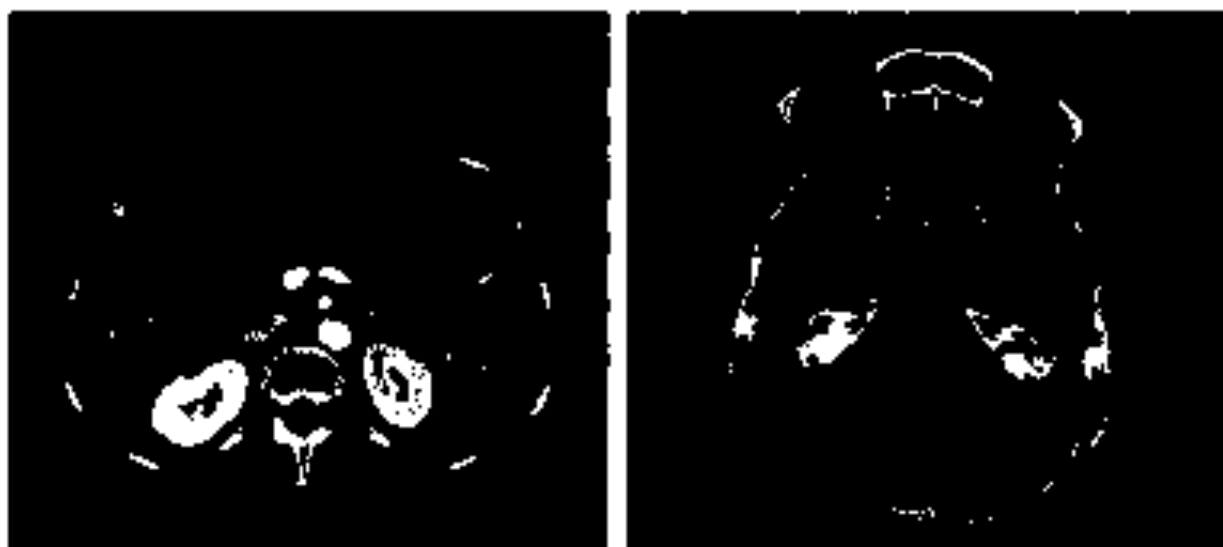


Fig. 1. CT-images of: (a) the abdomen, and (b) the base (base of the skull).

anatomical details, initial images show the clear and sharp resolution of fine bony structures and soft tissue anatomy free of image artifacts. Basically, this is the result of the properties of the CT X-ray scanning system together with the precise setting of the scan parameters and the image reconstruction algorithms.

1. Principle of computed tomography

The fundamentals of X-ray tomography were established by Hounsfield in 1972 [1]. The principle is based on the detection of a series of X-ray attenuation profiles from several different viewing directions, which subsequently allow the reconstruction of other sectional images of an object. A comprehensive introduction to CT-techniques and applications is given in refs. [2,3]. From a variety of technical systems for CT-scanners the so-called fan-beam design has proven to be the most advantageous. In fig. 2 a CT scanning system following the rotation-rotation principle is illustrated. In such a system, the X-ray tube and detector are rigidly coupled and rotate around the measurement field within a few seconds. A fan-shaped beam of X-rays continuously passes through a cross-sectional "slice" of the measurement field and hits the detector system. In order to be able to reconstruct CT images, attenuation profiles (projections) of that part of the patient's body located in the measurement field are scanned from several different viewing directions. The attenuation profiles are registered as a "single shot" for each viewing direction as an X-ray intensity pattern by

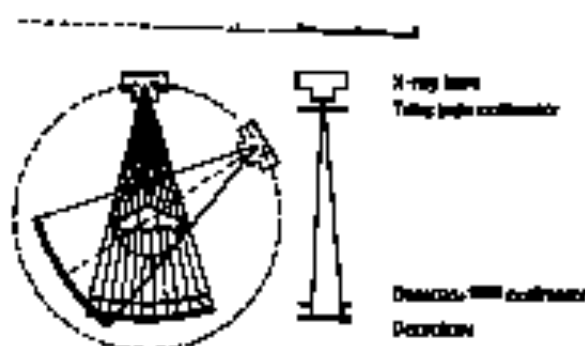


Fig. 2. Schematic system of X-ray computed tomography with fan-beam design and rotation-rotation principle [3].

means of a linear detector array system (see fig. 3). The detector array itself is built up of several hundreds of individual channels which generate the attenuation corresponding electrical signals. The width of the detector elements and the geometric arrangement of the X-ray source, collimator and detector determine the spatial distribution of the system which is presently about 60 mm.

Contrary to scintillation counting techniques, computed tomography X-ray detectors are operating in current mode due to the dose flux in the range of 1 R/s which yields quantum rates up to 10^{10} s^{-1} . Principally, the quantitative determination of X-ray intensities with a photon energy up to 150 keV can be realized by three detector types: semiconductor based detectors, ionization chambers and phosphor based detectors. In the case of semiconductor-based detectors, high-purity germanium is the favorite, but calls for thorough

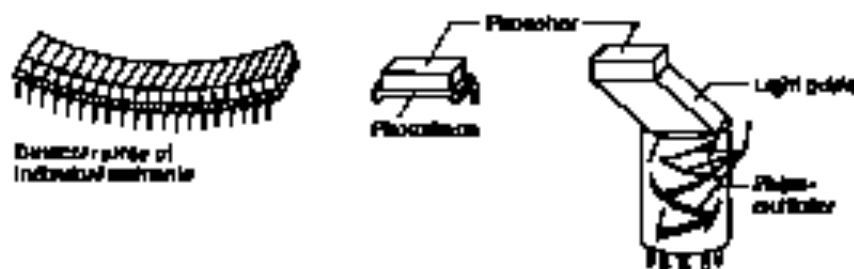


Fig. 3. Solid state detector module for X-ray computed tomography [4].

coupling [4] and its use is far from practical. In contrast, high pressure ionization detectors filled with argon are still today's dominating detector systems for CT. It gives excellent results but has its limitations, mainly in X-ray absorption and efficiency. Such gases, even when pressurized do not stop as many X-rays as solids, in particular those with high density, phosphors are of big interest. In general such detectors are realized by the combination of phosphors and photon detecting devices, such as photodiodes or -multipliers, as shown in fig. 3.

Modern CT scanners use detector arrays with at least 1000 individual X-ray detecting channels. Each detector element is about one millimeter wide. The spacing between the channels is rather small, but it proves to suppress cross talk by interchannels, to minimize the loss of dose utilization.

For solid-state detectors the phosphor-photodiode concept is preferred most. The X-rays absorbed by the phosphor are converted into visible radiation, which propagates to the photodiode coupled to the phosphor element on the side opposite to the incident X-ray. Thus, an electrical signal is generated by the photoelectric conversion of visible light. The following comments of this work refer to this detector principle.

3. Phosphor requirements

The CT-market offers different types of machines. Each type has its own principle and

therefore special properties and demands for the performance of components. Referring to solid-state detector systems, each principle has its individual advantages and disadvantages. For this reason the determination of the phosphor requirements for CT-application is limited to the principal physical and technical aspects. An overview of the most important properties is given in table 1 with the absorption, emission, optical and technical demands.

The key feature of CT is not the spatial resolution, but the contrast resolution which should have an accuracy of a few parts per thousand. Very small differences in X-ray absorption, which are in general a few percent for soft tissue parts, have to be detected precisely, while simultaneously CT must be able to detect the highest resolution in the case of bone material. With modern CT-techniques a few parts per thousand are recognized within a high dynamic range of up to 10^4 .

For phosphor based detectors the necessary high light output of the X-ray excited luminescence. Light output is therefore an overall universal measure due to the individuality of detector devices [6], but with respect to the phosphor, it is the result of X-ray absorption, efficiency of the internal luminescent processes and the interior optical quality to avoid losses of the excited light by scattering or absorption. Because the phosphor element is coupled to a photodiode, optical coupling of the emission wavelength should be close to the maximum of the diode's sensitivity to ensure high signal conversion. The phosphor has to show

Table 1
Basic requirements of phosphors for CT-applications

X-ray properties	Light emission	Optical properties	Technical notes
• Average atomic $Z > 30$	• Efficiency efficiency	• High transmission	• Noiseless
• Density $\rho \geq 2 \text{ g/cm}^3$	• High output	• Low scattering	• Chemical stability
• High surface stability	• Spectral matching (380-550 nm)		• Mechanical strength
	• Fast decay $< 0.1 \text{ ns}$		• Appended body
	• Blue emission $2 \text{ nm} < 0.3\%$		• Stochastic

high X-ray absorption for high dose utilization to avoid unnecessary radiation hazards to the patient. Therefore an average atomic number higher than about 50 or a density above 4 g/cm^3 is preferred.

Regarding the emission characteristics, high quantum- or radiant conversion efficiency is an essential demand. Although this is a basic physical "constraint" for a given phosphor, the preparation of the phosphor material has an important influence by controlling defect generation and impurity incorporation [7].

One of the primary requirements for suitable CT-phosphors is the rapid behavior of the emission after the termination of X-ray excitation. Afterglow, in particular, is an undesirable critical parameter. If the afterglow (scintillation) exceeds specific limitations, image degradation occurs due to memory effects. Such limitations are given by the scanning duration for CT imaging. The scan rate is determined by the need to avoid motion artefacts and to reduce exposure time for minimizing the patients' risk from the radiation hazard. For the fan-beam rotation-rotation principle a single rotation including up to 1500 projections takes, for example, two seconds. This yields time intervals of about 1.3 milliseconds for the read out of the detector channels. This time limit may give a qualitative measure of the time range of afterglow, with intensities of some parts per thousand. Due to the basic physical process of luminescence, decay time describes the behavior of the specific luminescent center while afterglow is asymptotic for a long time decrease by retardation effects.

Besides all these physical requirements the suitability of phosphors depends further on some technical aspects, for example, toxicity, chemical stability, reproducibility and machining possibilities. Finally, overall radiation stability is required. Nevertheless, for distinct phosphors extraordinary advantages may compete with some. In disadvantages so that comparison has to be considered.

4. Conventional single crystal phosphors

Within the period of technical developments of CT machines, phosphors for solid state detectors

have always been of interest. A detailed overview of the conventional phosphor systems has been given previously by Farahhi [8,9] and Chakraborty [7]. In table 2 the characteristic data of the most important phosphors are summarized together with some new scintillation-phosphors which are discussed in the following chapter. The alkali halides, tungstates and germanium-phosphors listed here, are single crystal type materials and are prepared by conventional crystal growth techniques.

For these phosphors only the main features are discussed. For further information refer to [7-9]. The X-ray excited emission spectra of some representative single crystal phosphors which exhibit broad band emission characteristics are plotted in fig. 4.

The thallium-doped alkali halides, NaI:Tl and CsI:Tl, are the most efficient known phosphors. In spite of high light output and short exponential decay, NaI:Tl is not applicable for CT use because of serious afterglow problem [8] and its hygroscopic nature. In contrast CsI:Tl is widely used in CT but still has several drawbacks. As shown in fig. 5 by dose dependent linearity measurements after X-ray excitation on cut, CsI:Tl shows a long afterglow. In addition its light output depends on its irradiation history, known as hysteresis and varies for different crystal facets. However, these difficulties may be controlled by pulsed CT techniques for detector calibration and by mathematical calculations.

With the tungstates, CaWO_4 and ZnWO_4 and $\text{Bi}_4\text{Ge}_2\text{O}_{12}$ (BGO) an excellent low afterglow is obtained (fig. 5). These materials like other unactivated phosphors have low radiant efficiency. Only the tungstates, where CaWO_4 is best, show a sufficient light output. Furthermore, tungstates have the tendency of cleavage parallel to distinct crystallographic planes, making precise machining of detector elements difficult; a drawback for their effective application to CT.

5. Recent developments

For the reason that CsI:Tl could be well suited for CT application, experiments were initiated to clarify if afterglow and hysteresis can be mini-

Table 2
Characteristic data of potential phosphors for CT-detectors.

	NaI:Tl	CsI:Tl	CdWO ₄	ZnWO ₄	Bi ₄ Ge ₃ O ₁₂	(Y, Gd) ₂ O ₃ :Eu	Gd ₂ O ₂ S:Pr,Ce,F
Type	single crystal	single crystal	single crystal	single crystal	single crystal	ceramic	ceramic
Structure	cubic	cubic	monoclinic	monoclinic	cubic	cubic	hexagonal
Density (g/cm ³)	3.67	4.52	7.99	7.87	7.13	(5.9)	7.34
Atten. coeff. 150 keV (cm ⁻¹)	2.20	3.21	7.93	7.80	9.93	(3.40)	6.86
Emission maximum (nm)	415	550	480	480	480	610	520
Light output 80 keV (rel.)	118	100	30	20	10	~40	~60
Decay time (μs)	0.23	0.98	5	5	0.3	~1000	~3
Afterglow (%)	90 (within 150 ms)	7-15 (after 20 ms)	2 (20 ms)	<1 (20 ms)	<1 (20 ms)	~700 (3 ms)	≤1 (3 ms)
Optical quality	clear	clear	clear	clear (coloured)	clear (colourless)	transparent	translucent
Chem. stability (attacked by)	Water (hygroscopic)	Water	HCl	HCl	Conc. HCl	Conc. HCl	HCl
Mechanical behavior (20°C)	brittle cleavable	plastic deformable	brittle cleavable	brittle cleavable	brittle	brittle high strength	brittle low strength

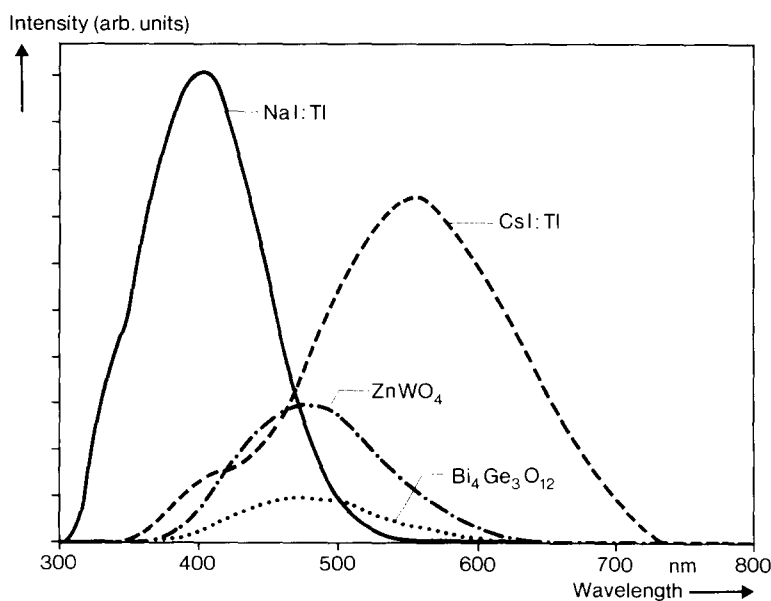


Fig. 4. X-ray excited emission spectra of various single crystal phosphors.

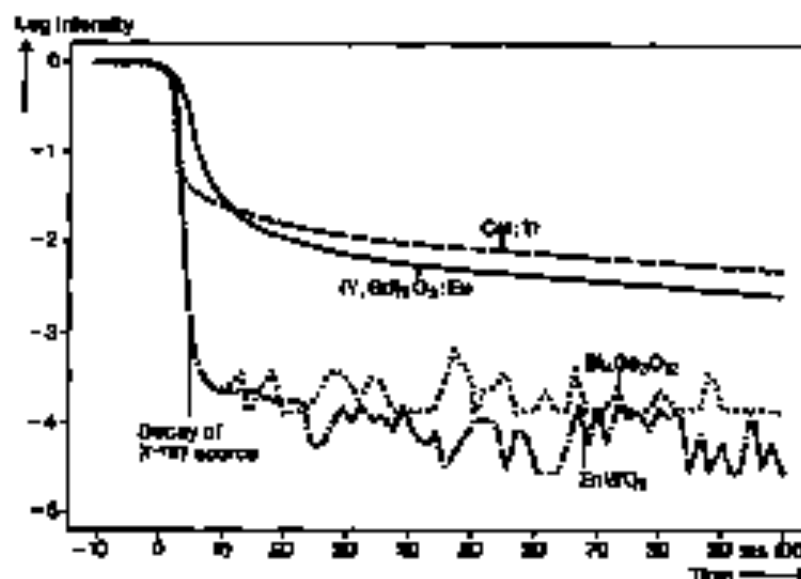


Fig. 5. Afterglow curves for various phosphors by X-ray excitation cell cell.

laid. An empirical study of the influence of crystal growth conditions, and selen/cadmium doping in particular, results in a slight improvement of the proportion mentioned above, however, radiant efficiency decreased markedly [10]. An analytical investigation of the radiation defects by optically detected magnetic resonance methods indicated that the interaction of V_L -vacancies and Tl -monomers as well as Tl -dimers very contribute to afterglow and hysteresis [11]. Further investigations are in progress to improve the understanding of the luminescent mechanisms.

For the last few years a new class of phosphors based on ceramic materials has been introduced by several groups for X-ray CT use [12]. These materials are derivatives of well known rare earth phosphor systems of oxides and oxynitrides which find new applications with the introduction of advanced ceramic technologies to phosphor preparation methods. Europium doped yttrium-gadolinium oxynitride, $Y_2O_3-Gd_2O_3:Eu$, and gadolinium oxynitride doped with praseodymium, cerium and thulium, $Gd_2O_3S:Pr,Ce,P$, are promising candidates of this class of phosphors as scintillators. The corresponding characteristics are listed in table 2 and the X-ray excited emission spectra

are illustrated in fig. 6. Values of table 2 are in brackets refer to a $Y_2O_3-Od_2O_3=2:1$ ratio and may be understood as an average value.

The rare earth ceramic phosphor, e.g. $Y_2O_3-Gd_2O_3:Eu$ containing more than 50 mole fractions of yttria to ensure cubic crystal structure, was developed by Cieskovich, Cumino et al. with special regard to CT applications (e.g. [13-16]). Using highly advanced ceramic sintering techniques, such as vacuum hot pressing or hot isostatic pressing with microwave or laser treatments, they obtained completely transparent, but polycrystalline ceramics. So, the problem of scattered light collection is well solved. The emission spectra during X-ray excitation (fig. 6) show the characteristic lines of the $Eu^{3+} D_2$ -multiplet to 7F_1 multiplet transitions. Light output, spectral sensitivity and technical properties exceed most of the single crystal phosphors. However, there is still an objection: long term afterglow (fig. 5) and even a long exponential decay time of about 1.3 milliseconds which is typical for Eu^{3+} -emission. Following the patent specifications this time behavior of the emission can be improved by additional doping with other rare earth ions or cerium with another valency. In the case of $Y_2O_3-Gd_2O_3:Eu$ the decay

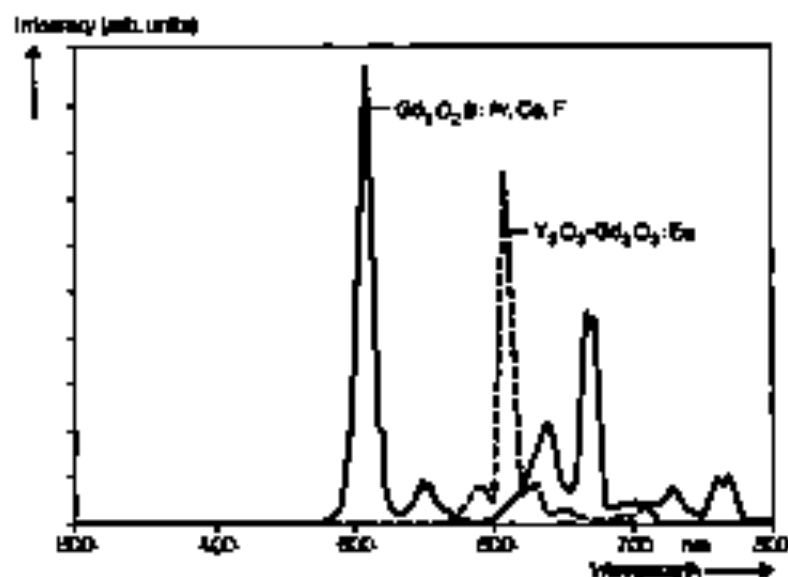


Fig. 6. X-ray excited emission spectra of nitrate phosphors.

time change from 1.3 ns to about 1.0 ns if ThO_2 is added [17]. This may be caused primarily by a reduction of the inversion symmetry of the surroundings of the Eu^{2+} -atom due to dopant and defect incorporation increasing the transition probability.

In contrast to the $\text{Y}_2\text{O}_3\text{-Gd}_2\text{O}_3\text{:Eu}$ phosphor, for $\text{Gd}_2\text{O}_2\text{S:Pr,Ce,F}$ a very low afterglow is reported [18]. This ceramic phosphor established by Yamada, Tanaka et al. is made from a gas derived phosphor powder by hot isostatic pressing using some sintering aids [18-20]. By this technique a highly densified ceramic with a residual porosity of less than 1% is obtained. Due to the hexagonal crystal structure of this compound only transparency is achievable. In spite of this principal limitation of the optical quality high light output is achieved. The X-ray excited emission exhibits the characteristic Pr^{3+} transitions from the $^3\text{P}_2$ manifold and $^1\text{D}_2$ to the $^3\text{H}_4$ manifold ground state. Typically Pr^{3+} shows a very rapid decay.

To assure low afterglow the Ce- and F-dopants are introduced. It was found that doping with F decreases the afterglow by about one order of magnitude. As shown by the thermoluminescence glow curve in fig. 7, this effect is attributed to a stabilization of the deep trap states while low traps

at about 260 K are destabilized. In addition Ce-doping decreases the concentration of all trap states observed [20].

4. Conclusion and future work

At present, the "ideal" phosphor for CT detectors is not available. For CT-application compromises are still necessary. With the recently developed ceria based rare earth phosphors, like $\text{Y}_2\text{O}_3\text{-Gd}_2\text{O}_3\text{:Eu}$ and $\text{Gd}_2\text{O}_2\text{S:Pr,Ce,F}$, further progress may be achievable by offering increased light output, higher stability and lower afterglow. Although these "new" phosphors are derivatives of well known phosphor systems, the advanced ceramic technologies allow the preparation of compact phosphor elements, even with high optical quality, of materials where single crystals are not available. As a sophisticated approach to phosphor engineering the ceramic way may give new possibilities. In the case of phosphor activation by multicomponent doping, ceramic preparation methods may offer more flexibility than crystal growth techniques as dopant incorporation easily occurs by solid state reactions. Thus, controlled sintering of the phosphors chemical and

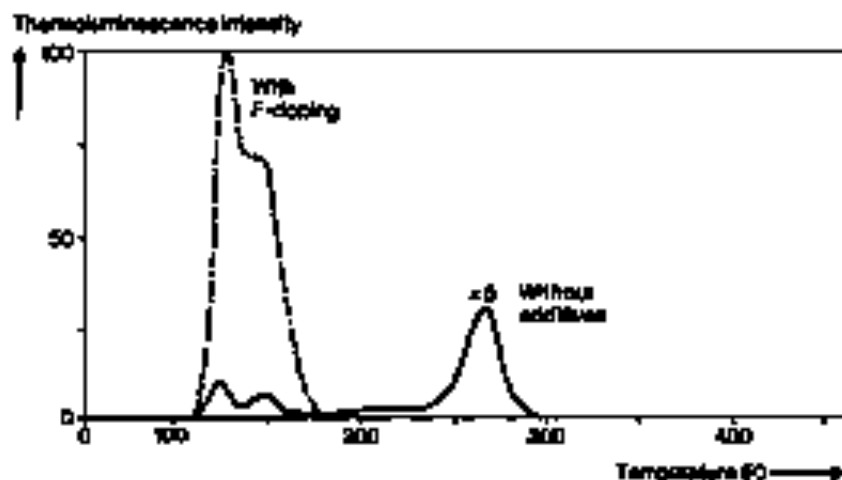


Fig. 7. Influence of F-doping on TML thermoluminescence glow curve of $\text{Ga}_2\text{O}_3\text{:Fe}$ [20].

structural properties, including lattice defects, should result in improved phosphor properties.

Future phosphors may prove to be either rare earth systems [21] and so far undiscovered compounds. However, the development of these phosphors will call for a considerable effort in science and technology with an accurate understanding of the basic physics. In the case of phosphors for high performance CT-use the mechanism of after-glow which is mostly of nonexponential, mixed nature is of special interest.

Acknowledgement

The authors wish to thank W. Böhner for valuable discussion and W. Köder for decay measurements.

References

- [1] E.M. Novotny, *ib. J. Nucl. En.* 36 (1973) 1016.
- [2] J. Alexander, *Computer Tomography*, Walter de Gruyter Verlag (Ain-Verl) (1985).
- [3] J. Alexander and K.-J. Krause, *Electronvol. 36* (1986) 58.
- [4] P.A. Glasow, J. Clarend, K. Kallig and W. Lichtenberg, *IEEE Trans. Nucl. Sci.* NS-28 (1981) 563.
- [5] P. Koll, *Phys. Bl. 34* (1981) 2.
- [6] I. Hill, E. Lorenz and G. Mägder, *IEEE Trans. Nucl. Sci.* NS-28 (1980) 105.
- [7] B.C. Grabovater, *IEEE Trans. Nucl. Sci.* NS-31 (1984) 372.
- [8] M.E. Furek, *Workshop on Tomography and Electron Comp. Tomogr., Seoul, Korea* (1978).
- [9] M.M. Fakhri, *IEEE Trans. Nucl. Sci.* NS-29 (1982) 1270.
- [10] B.C. Grabovater and W. Bausner, unpublished results.
- [11] W. Matus and M.D. Spach, to be published.
- [12] K. Yoshik, N. Inamura and M. Takami, *J. Electrochem. Soc.* 135 (1988) 907.
- [13] C.D. Grabovater, D.A. Casani and P.A. Dillman, *US Pat. 4,318,348* (1979).
- [14] F.A. Dillman, L.P.J. Georges, D.A. Casani and C.D. Grabovater, *US-Pat. 4,325,408* (1985).
- [15] C.D. Grabovater, D.A. Casani and P.A. Dillman, *US Pat. 4,371,332* (1985).
- [16] D.A. Casani, C.D. Grabovater and F.A. Dillman, *ED-Pat. 0 997265*.
- [17] W. Matus, M.D. Spach, B.C. Grabovater and W. Bausner, unpublished results.
- [18] Y. Doi, H. Yamada, M. Yoshida, H. Fujii, O. Tada, M. Takachi and Y. Tsubota, *Jpn. J. Appl. Phys.* 27 (1988) L1371.
- [19] M. Yoshida, N. Nakagawa, H. Fujii, F. Kawaguchi et al., *Jpn. J. Appl. Phys.* 27 (1988) L1572.
- [20] M. Yamada, A. Sasaki, Y. Uchida, M. Yamada, D. Yuzumoto and Y. Tsubota, *J. Electrochem. Soc.* 136 (1989) 2713.
- [21] G. Blasse, *Nat. Chem. Phys.* 16 (1987) 201.